

Unique $[\infty\text{Ni}_8\text{Bi}_8\text{S}]$ Metallic Wires in a Novel Quasi-1D Compound. Synthesis, Crystal and Electronic Structure, and Properties of $\text{Ni}_8\text{Bi}_8\text{SI}$

Alexey I. Baranov,[†] Lars Kloo,[‡] Andrei V. Olenov,[§] Boris A. Popovkin,^{*,§} Anatolii I. Romanenko,[⊥] and Andrei V. Shevelkov[§]

Contribution from the Department of Materials Science, Moscow State University, Vorob'evy Gory, Moscow 119899, Russia, Inorganic Chemistry, Royal Institute of Technology, Stockholm S 100 44, Sweden, Department of Chemistry, Moscow State University, Vorob'evy Gory, Moscow 119899, Russia, and Inorganic Chemistry Institute, Siberian Branch of RAS, Novosibirsk, Russia

Received July 24, 2001

Abstract: A new quasi-one-dimensional compound $\text{Ni}_8\text{Bi}_8\text{SI}$ has been synthesized and its crystal structure determined from single-crystal X-ray diffraction data. The structure of $\text{Ni}_8\text{Bi}_8\text{SI}$ consists of $[\infty\text{Ni}_8\text{Bi}_8\text{S}]$ columns separated by iodine atoms. Conductivity and magnetic susceptibility measurements (down to 4.2 K) show that $\text{Ni}_8\text{Bi}_8\text{SI}$ is a one-dimensional metal and exhibits Pauli paramagnetic properties. These observations are in good agreement with the results from electronic structure calculations. An analysis of the chemical bonding employing difference electron charge density maps reveals strong multicenter Ni–Bi bonds and pair Ni–S interactions within the $[\infty\text{Ni}_8\text{Bi}_8\text{S}]$ columns. Only electrostatic interactions are inferred between the columns and iodine atoms.

Introduction

Low-dimensional systems of metallic bonds have been attracting great interest from chemists and physicists for several decades.¹ Among these systems, one-dimensional polyhedral columns of metal atoms represent a family of less-studied compounds. Separate columns of metal atoms are observed only in two types of phases. They are the so-called condensed Chevrel phases² of a generic formula MMO_3Ch_3 ($M = \text{K, Rb, Cs, Tl, In}$; $\text{Ch} = \text{S, Se}$) and tantalum/niobium ternary tellurides $\text{M}_4\text{Te}_4\text{E}^{3-5}$ ($M = \text{Nb, Ta}$; $\text{E} = \text{Al, Si, Cr, Fe, Co, Ni}$). Also known are the phases in which similar columns are joined into three-dimensional networks, e.g. Ta_3S_2 ,⁶ Y_4OsBr_4 ,⁷ and $\text{Ta}_{11}\text{Si}_2\text{Se}_8$.⁸

The core of a 1D column in the examples mentioned consists of early 4d or 5d metals having quite a small number of valence electrons. Such a core is enveloped by chalcogen atoms. In Nb and Ta tellurides a light element atom resides in the center of the metal polyhedron.

Here, we report the first one-dimensional compound $\text{Ni}_8\text{Bi}_8\text{SI}$ of a new type of low-dimensional compounds, in which

conducting metal columns are separated by insulating I^- anions. The core of the metallic column is made of Ni atoms forming square antiprisms, surrounded by Bi atoms, and with S atoms in every second Ni_8 antiprism. The title compound was unexpectedly obtained during an attempt to grow crystals of $\text{Ni}_{11}\text{Bi}_5\text{S}_4$,⁹ a possible new low-dimensional conducting material, by chemical transport reaction with I_2 using the stoichiometrically annealed charge. In this paper we discuss the crystal and electronic structure and physical properties of $\text{Ni}_8\text{Bi}_8\text{SI}$.

Experimental Section

Synthesis. $\text{Ni}_8\text{Bi}_8\text{SI}$ was synthesized by annealing the stoichiometric mixture of elements (Ni 99.99 Aldrich, Bi 99.99, S 99.99, I_2 99.99) in an evacuated quartz ampule at 530 °C (170 h) followed by grinding and further annealing under the same conditions. A black solid of intergrown, needle-shaped crystals formed in the course of synthesis. The X-ray powder pattern (Cu $\text{K}\alpha_1$ radiation, STADI/P (Stoe)) showed excellent agreement with the theoretical pattern generated from the single-crystal X-ray diffraction data (see below); no impurities were found. The substance is stable in air.

To obtain good single crystals for the crystal structure determination and physical properties measurements, the sample synthesized (approximately 0.4 g) was placed in a quartz tube (1.2×10 cm) together with I_2 (approximately 0.03 g), which was evacuated and sealed off. The growth was carried out in a horizontal gradient furnace at 570 (at the sample) and 500 °C (at the empty end of the ampule) over 170 h. Needle-shaped black crystals were found in the “cold” part of the ampule.

Crystal Structure Determination. A suitable single crystal was mounted on a CAD4 (Nonius) goniometer head for the structure determination. Mo $\text{K}\alpha$ radiation and a graphite monochromator were used. The tetragonal unit cell was refined based on 24 well-centered reflections in the angular range $12.28^\circ < \theta < 13.25^\circ$. The data set was collected at ambient temperature in an ω - 2θ mode with the data collection parameters listed in Table 1. A semiempirical absorption correction was applied to the data based on ψ -scans of 4 reflections

* Address correspondence to this author: (phone) +7-095-939-3339; (fax) +7-095-939-0171; (e-mail) popovkin@inorg.chem.msu.ru.

[†] Department of Materials Science, Moscow State University.

[‡] Royal Institute of Technology.

[§] Department of Chemistry, Moscow State University.

[⊥] Inorganic Chemistry Institute.

(1) Rouxel, J. *Acc. Chem. Res.* **1992**, 25, 328.

(2) (a) Huster, J.; Schippers, G.; Bronger, W. *J. Less-Common Met.* **1983**, 91, 333. (b) Potel, M.; Chevrel, R.; Sergent, M. *Acta Crystallogr. B* **1980**, 36, 1545.

(3) Neuhausen, J.; Finckh, E. W.; Tremel, W. *Chem. Ber.* **1995**, 128 (6), 569.

(4) Badding, M. E.; DiSalvo, F. J. *Inorg. Chem.* **1990**, 29 (20), 3952.

(5) Badding, M. E.; Gitzendanner, R. L.; Ziebarth, R. P.; DiSalvo, F. J. *Mater. Res. Bull.* **1994**, 29 (3), 327.

(6) Kim, S.-J.; Nanjundaswamy, K. S.; Hughbanks, T. *Inorg. Chem.* **1991**, 30, 159.

(7) Dorhout, P. K.; Corbett, J. D. *J. Am. Chem. Soc.* **1992**, 114, 1697.

(8) Mrotzek, A.; Harbrecht, B. *Eur. J. Inorg. Chem.* **1999**, 87–93.

(9) Mariolacos, K. *Chem. Erde* **1987**, 46 (3–4), 315.

Table 1. Crystallographic Data for Ni₈Bi₈SI

formula	Ni ₈ Bi ₈ SI
formula mass (amu)	2300.23
space group	<i>P4</i> (No. 75)
<i>a</i> (Å)	9.774(1)
<i>c</i> (Å)	4.197(1)
volume (Å ³)	401.0(5)
<i>Z</i>	1
<i>T</i> (K)	293
θ_{\max} (deg)	27.99
ρ_{calcd} (g cm ⁻³)	9.526
μ (mm ⁻¹)	98.558
goodness-of-fit, all data	1.018
largest diff peak and hole (eÅ ⁻³)	4.688 and -5.455
no. of measd/independent/parameters	608/549/43
<i>R</i> (<i>F</i>) for $F_o > 4\sigma(F_o^2)^a$	0.0671
<i>R</i> _w (F_o^2) ^b	0.1594

^a $R(F) = \{\sum||F_o| - |F_c||\} / \{\sum|F_o|\}$. ^b $w = 1/[\sigma^2(F_o^2) + (0.1030P)^2]$ where $P = (F_o^2 + 2F_c^2)/3$.

Table 2. Positional and Thermal Parameters for Ni₈Bi₈SI

	Wyckoff	<i>x/a</i>	<i>y/b</i>	<i>z/c</i>	U ^{eq}
Bi(1)	4(d)	0.8762(1)	0.3590(1)	0.528(1)	0.0167(5)
Bi(2)	4(d)	0.6604(1)	0.1737(1)	0.030(1)	0.0169(6)
Ni(1)	4(d)	0.0888(6)	0.1829(6)	0.524(4)	0.012(1)
Ni(2)	4(d)	0.9371(6)	0.1935(6)	0.040(4)	0.016(1)
S	1(a)	0	0	0.790(6)	0.002(4)
I	1(b)	1/2	1/2	0.563(9)	0.064(4)

having their χ angles close to 90°. An analysis of the data collected showed the absence of systematic extinctions. The space group *P4* (no. 75) was chosen for the structure solution. The positions of bismuth and iodine atoms were found from direct methods (SHELXS-97¹⁰). Nickel and sulfur atoms were localized by a sequence of least-squares cycles and $\Delta\rho(xyz)$ syntheses. The absence of correlations between atomic coordinates confirmed the choice of the space group. An attempt to solve the crystal structure in the centrosymmetric space group *P4/m* failed, thus confirming the right choice of the noncentrosymmetric space group. The final anisotropic refinement on *F*² (SHELXL-97¹⁰) led to *R*₁ = 0.0671. Atomic positions and thermal parameters are listed in Table 2.

Measurements of Properties of Ni₈Bi₈SI

(a) **Thermal Properties.** The pure substance was placed in a small quartz ampule, which was evacuated and sealed off. The differential thermal analysis curve was recorded at 5 °C/min heating rate.

(b) **Resistivity Measurements.** The electrical resistivity of a small crystal (needle, length 1 mm, thickness 0.01 mm) was measured parallel to the needle axis in the temperature range 4.2–600 K employing the standard four-probe technique with use of silver paste contacts. The contact resistivity was found to be ohmic and about 1 Ohm.

(c) **Magnetic Susceptibility Measurements.** A small amount (0.004 g) of the ground single crystals of Ni₈Bi₈SI was placed in a plastic capsule. The magnetic susceptibility was measured with the use of an MPMS2 SQUID (Quantum Design) magnetometer in the temperature range of 4.2–100 K.

Calculation Details

General. The electronic structure of Ni₈Bi₈SI was calculated with the use of the CRYSTAL98¹¹ program package. The Hay–Wadt effective core potential (ECP) and basis set,¹² which had to be modified (see below), were used for calculations (B3LYP exchange-correlation

potential). The Hartree–Fock and DFT [local density approach (LDA) with the Vosko–Wilk–Nusair exchange correlation potential (VWN)] Hamiltonians were used to check the dependence of the results on the Hamiltonian model used. A mesh of 28 k-points was used in calculations. The analysis and visualization of difference electronic charge densities were performed with use of the TOPOND98¹³ and gOpenMol¹⁴ program packages.

Basis Set and ECP. To make the Hay–Wadt basis set and ECP applicable for calculations of extended systems, several modifications were made. The *f*–*g* term of the original ECP for Bi¹² was eliminated (CRYSTAL98 does not handle orbitals with *l* > 2). One too diffuse exponent (<0.1) of a *p*-type Gaussian in the original Bi basis set¹² was removed, and the contraction was completely split to provide a basis set flexibility. Our test calculation of bulk bismuth metal showed the modified basis set to give realistic properties (DFT calculations within the Vosko–Wilk–Nusair exchange-correlation potential in agreement with ref 15).

The smallest *s*- and *p*-exponents of the original basis sets¹² for S and I were uncontracted (their coefficients were allowed to vary) to provide a higher degree of basis set flexibility. These modified basis sets have been proven to perform well in other calculations carried out in our group.

An additional *d*-exponent of value 0.20 was added to the modified Hay–Wadt small-core basis set.¹⁶ After this modification, the electronic structure of the bulk nickel (both para- and ferromagnetic) was represented well, in good agreement with the results of ref 17.

Results

Crystal Structure. Ni₈Bi₈SI is made of [_∞Ni₈Bi₈S] one-dimensional infinite columns and rows of iodine atoms packed in a square manner (Figure 1). Square antiprisms of Ni₈ share common square faces forming the infinite columns running parallel to the crystallographic *c*-axis. The Bi atoms reside close to the edges of each Ni₄ square. The sulfur atoms are situated approximately at the centers of the Ni₈ antiprisms, occupying half of them in a regular way (every second).

The interatomic distances fall in the following ranges: Ni–Bi 2.679(1)–2.753(1) Å, Ni–Ni 2.519(1)–2.810(8) Å, and Ni–S 2.248(1)–2.279(1) Å. The Ni–Bi separations are the same as those observed in NiBi₃¹⁸ and NiBi.¹⁹ The Ni–Ni is only slightly longer in distance than in Ni metal,²⁰ 2.49 Å, while the Ni–S contacts are typical for binary sulfides, such as Ni₃S₂²¹ or NiS²² (2.25–2.40 Å). The shortest Bi–Bi separations of 3.487(6)–3.646(5) Å are significantly longer than in discrete bismuth clusters²³ (3.0–3.3 Å). The iodine atoms are surrounded by 12 bismuth atoms, the Bi–I contacts being 3.930(2)–4.06(1) Å. These are significantly longer than in mixed nickel–bismuth iodides²⁴ (3.3–3.5 Å) and Bi binary iodides (3.0–3.3 Å).²⁵

(13) Gatti, C. *TOPOND 98 User's Manual*; CNR-CSR SRC: Milano, 1999.

(14) Laaksonen, L. *gOpenMol*, version 1.4: <http://www.csc.fi/~laaksonen/gopenmol/gIntro.html>.

(15) Shick, A.; Ketterson, J. B.; Novikov, D. L.; Freeman, A. J. *Phys. Rev. B* **1999**, *60* (23), 15484.

(16) Freyria-Fava, F. Thesis, Turin, 1997.

(17) Jarlborg, T.; Freeman, A. J. *J. Magn. Magn. Mater.* **1980**, *22*, 6.

(18) Ruck, M. Habilitationsschrift, University of Karlsruhe, Karlsruhe, 1997.

(19) Ruck, M. *Z. Anorg. Allg. Chem.* **1999**, *625*, 2050.

(20) Swanson, H. E.; Tatge, E. *Natl. Bur. Stand. (U.S.)* **1953**, Circular 539, 13.

(21) Parise, J. B. *Acta Crystallogr. B* **1980**, *36*, 1179.

(22) Rajamani, V.; Prewitt, C. T. *Can. Mineralog.* **1974**, *12*, 253.

(23) (a) Von Schnering, H. G.; von Benda, H.; Kalveram, C. *Z. Anorg. Allg. Chem.* **1978**, *438*, 37. (b) Beck, J.; Brendel, C. J.; Bengtsson-Kloo, L.; Krebs, B.; Mummert, M.; Stankowski, A.; Ulvenlund, S. *Chem. Ber.* **1996**, *129*, 1219.

(24) (a) Ruck, M. *Z. Anorg. Allg. Chem.* **1995**, *621* (12), 2034. (b) Ruck, M. *Z. Anorg. Allg. Chem.* **1997**, *623* (2), 243.

(25) Trotter, J.; Zobel, T. *Z. Kristallogr.* **1966**, *123*, 67.

(10) (a) Sheldrick, G. M. *SHELXS-97*, Program for crystal structure solution; University of Göttingen: Göttingen, Germany, 1997. (b) Sheldrick, G. M. *SHELXL-97*, Program for crystal structure refinement; University of Göttingen: Göttingen, Germany, 1997.

(11) Saunders, V. R.; Dovesi, R.; Roetti, C.; Causà, M.; Harrison, N. M.; Orlando, R.; Zicovich-Wilson, C. M. *CRYSTAL98 User's Manual*; University of Torino: Torino, 1998.

(12) Hay, P. J.; Wadt, W. R. *J. Chem. Phys.* **1985**, *82* (1), 270.

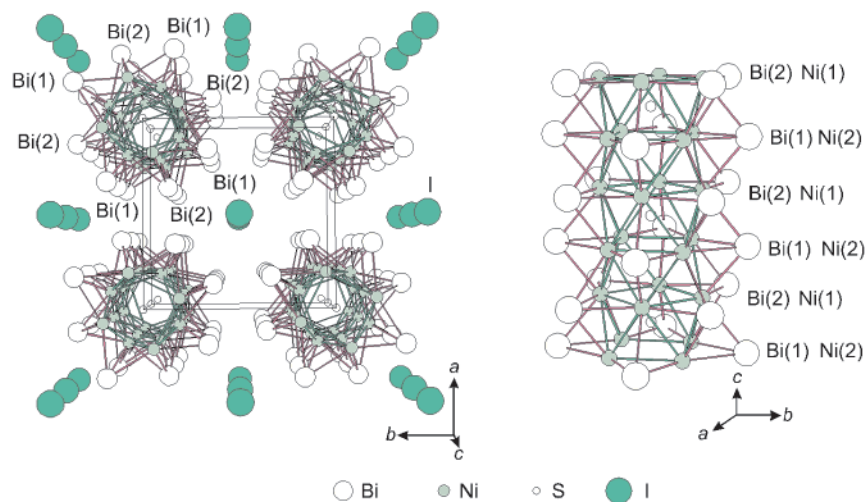


Figure 1. The crystal structure of $\text{Ni}_8\text{Bi}_8\text{SI}$. A perspective view along the c -axis (left) and the fragment of the $[\infty\text{Ni}_8\text{Bi}_8\text{S}]$ column (right).

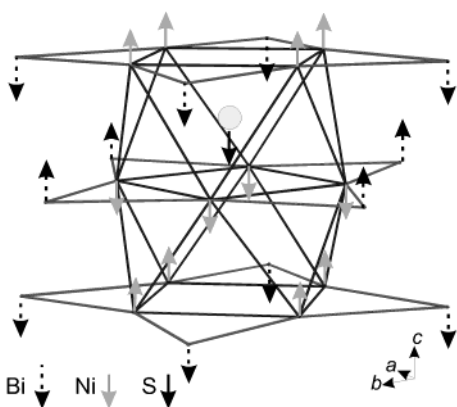


Figure 2. Distortion of the $[\infty\text{Ni}_8\text{Bi}_8\text{S}]$ column. The directions of the distortion are shown by arrows.

The units (i.e. antiprisms) of the $[\infty\text{Ni}_8\text{Bi}_8\text{S}]$ columns are not equivalent. The “heights” of the antiprisms with and without S inside are different: the former type is “taller” than the latter by approximately 0.13 Å. In addition, the Bi atoms are slightly shifted (approximately 0.02–0.04 Å) out of the plane of the square face of the Ni_8 antiprism toward the S atoms as can be seen in the atomic coordinates (Table 2). Furthermore, the S atoms are not exactly located in the center of the Ni_8 antiprisms, but are shifted by 0.07 Å (Figure 2). Consequently, $\text{Ni}_8\text{Bi}_8\text{SI}$ crystallizes in a noncentrosymmetric space group.

Physical Properties: (a) **Thermal properties:** Two resolved endothermic effects at 596 ± 5 and 601 ± 5 °C were registered in the DTA experiment (heating mode). Together with the visual observation of the solidified melt upon cooling this indicates a peritectical melting of $\text{Ni}_8\text{Bi}_8\text{SI}$.

(b) **Electrical properties:** The compound has a metallic type of conductivity (Figure 3). The resistivity at room temperature was found to be $\rho_{\text{II}}(300) = 30 \mu\Omega \text{ cm}$. The temperature dependence of the resistivity $\rho_{\text{II}}(T)$ can be approximated in the range 4.2–50 K by the dependence

$$\rho_{\text{II}}(T) = \rho_0 + kT^2 \quad (1)$$

where $\rho_0 = 1.05825 \mu\Omega \text{ cm}$ and $k = 0.00112401 \mu\Omega \text{ cm K}^{-2}$. Such dependence is characteristic of quasi-one-dimensional conductors.²⁶ At higher temperatures the resistivity increases linearly up to 600 K.

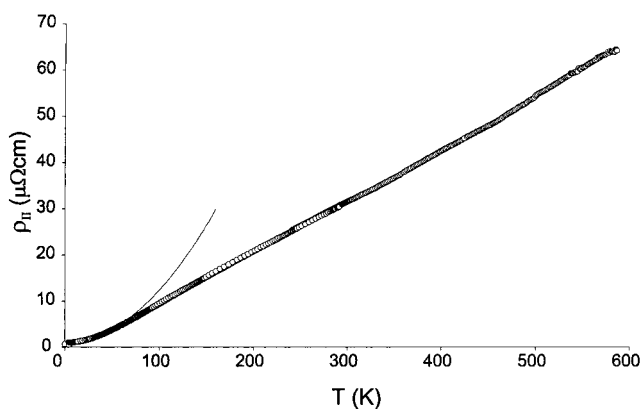


Figure 3. Temperature dependence of resistivity, $\rho_{\text{II}}(T)$, in the temperature range 4.2–600 K. The solid curve is a low-temperature fit according to eq 1.

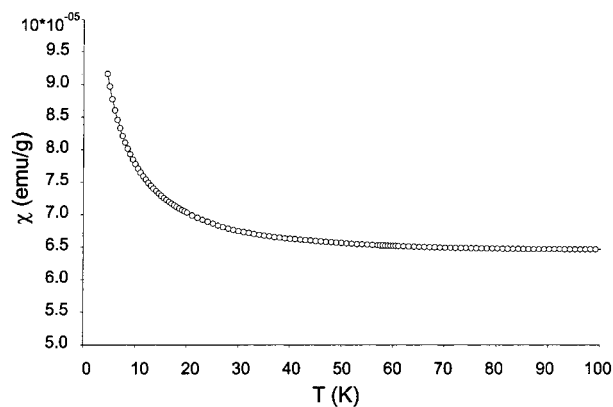


Figure 4. Temperature dependence of the magnetic susceptibility, $\chi(T)$, in the temperature range 4.2–100 K.

(c) **Magnetic properties:** The susceptibility curve is shown in Figure 4, being $\chi(77 \text{ K}) = 6.5 \times 10^{-5} \text{ emu/g}$. $\text{Ni}_8\text{Bi}_8\text{SI}$ exhibits a temperature-independent Pauli paramagnetism. The raise of susceptibility below about 40 K is caused by paramagnetic impurities and the container material.

Electronic Structure and Bonding. The calculated total density of states (DOS) and the band structure are presented in Figure 5. According to the bands close to the Fermi level, $\text{Ni}_8\text{Bi}_8\text{SI}$ should have metallic properties of strong anisotropy. The bands providing the conductivity (i.e. in the proximity of the Fermi level) are mainly composed of Bi p- and Ni d-orbitals.

(26) Oshiyama, A.; Nakao, K.; Kamimura, H. *J. Phys. Soc. Jpn.* **1978**, 45 (4), 1136.

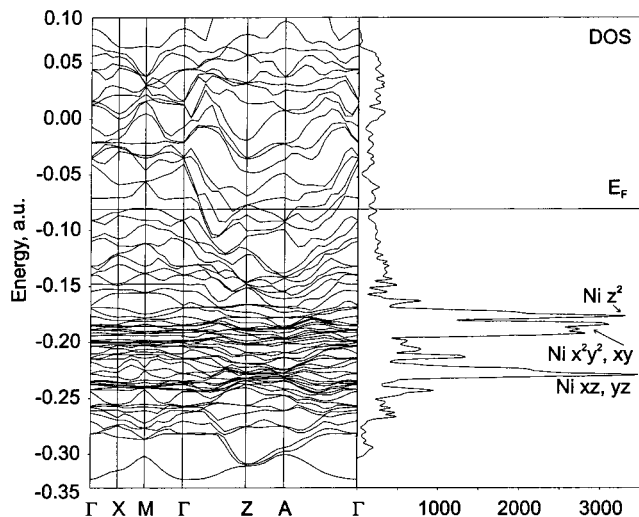


Figure 5. Band structure and total density of states for $\text{Ni}_8\text{Bi}_8\text{SI}$.

While there are two crystallographically nonequivalent Ni and Bi atoms, their projected DOS (pDOS) curves are very similar. The DOS in the energy range shown in Figure 5 displays two strong peaks. The analysis of the pDOS of the elements shows that they essentially correspond to Ni d-orbitals. The splitting of these peaks corresponds to Ni–S bonding/Ni–Bi nonbonding (the lower) and Ni–S nonbonding/Ni–Bi bonding (the higher) combinations. The Ni d-orbital angular components are shown in Figure 5. The bonding character of the bands was revealed by the analysis of the difference electron charge densities (see below).

The comparison between the pDOS and the occupancy level shows that the Ni d-based orbitals are almost fully occupied, as well as the Bi, S, and I s-orbitals. The p-orbitals of Bi are approximately half-filled. The p-orbitals of S and I are essentially fully occupied, whereas the Ni s- and p-orbitals are close to empty.

Since the Ni d-states are almost completely filled, $\text{Ni}_8\text{Bi}_8\text{SI}$ should be Pauli paramagnetic. That is in a good agreement with the magnetic measurement data.

The difference electron charge density ($\Delta\rho$, defined as a calculated charge density minus the superposition of atomic charge densities) was visualized to analyze a real-space representation of the bonding in $\text{Ni}_8\text{Bi}_8\text{SI}$. Maxima of the difference electron charge density can be observed as isosurfaces. Such maxima could be interpreted as centers of regions where the chemical bonds are located. In terms of the topology of the difference charge density gradient field, they can be called attractors in accordance with the terminology usually employed in the analysis of the charge density gradient field.²⁷ The difference charge density maps of $[\infty^1\text{Ni}_8\text{Bi}_8\text{S}]$ are presented in Figure 6. The levels of isosurface ($\Delta\rho$ value) were chosen to clearly display all maxima.

The strongest interaction can be observed as thick rods (marked A in Figure 6). They correspond to 5-center (4Ni + Bi) interactions, and since the crystal structure has two nonequivalent Bi atoms, there are two types of maxima A1 and A2. One can observe a slight difference in shape between these two maxima. The maxima of the type B seem to correspond to a 5-center (Bi4 + Ni) interaction. Again, there are two types of such maxima with different shapes.

The maxima of type C correspond to pairwise Ni–S interactions. Eight such maxima with a disk shape can be

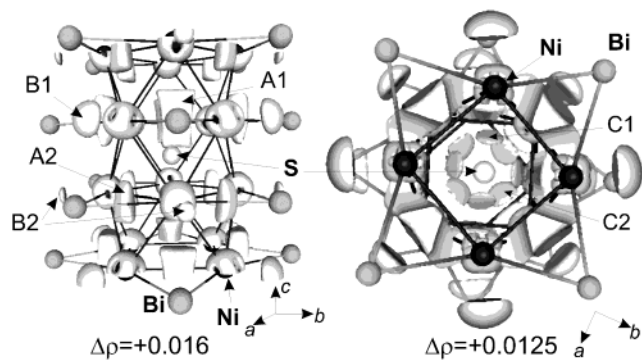


Figure 6. Calculated difference charge density (of level shown in $e^- \text{au}^{-3}$) in the $[\infty^1\text{Ni}_8\text{Bi}_8\text{S}]$ column.

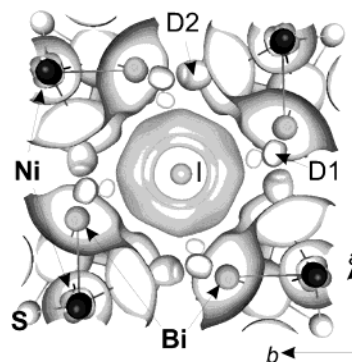


Figure 7. Difference charge density ($\Delta\rho = +0.01 e^- \text{au}^{-3}$) in $\text{Ni}_8\text{Bi}_8\text{SI}$ close to the I^- anion.

observed surrounding the S atom inside the square antiprisms of the Ni atoms. The difference between the C1 and C2 maxima is less pronounced.

Figure 7 illustrates the difference charge density close to the I atom. The interaction between the iodine and $[\infty^1\text{Ni}_8\text{Bi}_8\text{S}]$ columns appears to be predominantly electrostatic, since the isosurface has essentially a spherical shape. A Mulliken charge analysis shows that the iodine essentially can be regarded as I^- anions, and hence the $[\infty^1\text{Ni}_8\text{Bi}_8\text{S}]^+$ entity should have the charge +1. Also, the lone s-pairs of the Bi atoms can be observed in Figure 7 (labeled D1 and D2).

In summary, the most important stabilizing interactions in $\text{Ni}_8\text{Bi}_8\text{SI}$ are multicenter interactions between Ni and Bi, and two-center Ni–S interactions within the $[\infty^1\text{Ni}_8\text{Bi}_8\text{S}]^+$ columns. An electrostatic interaction then ties the 1D charged columns and I^- anions together.

Discussion

The compound $\text{Ni}_8\text{Bi}_8\text{SI}$ represents a novel type of one-dimensional metallic conductor. However, the principal building unit, the $[\infty^1\text{Ni}_8\text{Bi}_8\text{S}]$ column, resembles strongly $\text{M}_4\text{Te}_4\text{E}$ columns found in a series of isostructural compounds Ta_4FeTe_4 ,³ $\text{Ta}_4\text{Te}_4\text{Ni}$, $\text{Ta}_4\text{Te}_4\text{Al}$, Ta_4SiTe_4 ,⁴ $\text{Nb}_4\text{Te}_4\text{Si}$, $\text{Nb}_4\text{Te}_4\text{Fe}$, $\text{Nb}_4\text{Te}_4\text{Co}$, $\text{Ta}_4\text{Te}_4\text{Cr}$, and $\text{Ta}_4\text{Te}_4\text{Co}$.²⁸ It is thus appropriate to discuss the crystal and electronic structure and properties of the title compound in comparison with the Nb and Ta ternary tellurides.

In the reported crystal structures of $\text{Ta}_4\text{Te}_4\text{E}$ (E = Si, Fe), the Ta atoms form almost regular square antiprisms sharing common square faces, in a similar way as the Ni atoms in the crystal structure of $\text{Ni}_8\text{Bi}_8\text{SI}$. The Te atoms reside around the Ta_4 squares such as the Bi atoms in $\text{Ni}_8\text{Bi}_8\text{SI}$ do. In contrast to

(27) Bader, R. W. F. *Atoms in molecules. A quantum theory*; Clarendon Press: Oxford, 1990.

(28) Ahn, K.; Hughbanks, T.; Rathnayaka, K. D. D.; Naugle, D. G. *Chem. Mater.* **1994**, *6*, 418.

$\text{Ni}_8\text{Bi}_8\text{SI}$, the Si or Fe atoms in the tantalum tellurides are trapped in the center of the Ta_8 antiprisms and form almost linear chains with short Si–Si or Fe–Fe contacts. In this way, the linear columns $[^1_{\infty}\text{Ta}_4\text{Te}_4\text{E}]$ are formed in those compounds. Unlike $\text{Ni}_8\text{Bi}_8\text{SI}$, $\text{Ta}_4\text{Te}_4\text{Fe}$ and $\text{Ta}_4\text{Te}_4\text{Si}$ crystallize in centrosymmetric space groups, and consequently no distortions of the columns exist in those phases. Also, the way these columns are packed in the crystal structures of $\text{Ta}_4\text{Te}_4\text{E}$ differs from the situation in $\text{Ni}_8\text{Bi}_8\text{SI}$ and exhibits a hexagonal array in contrast to the square array in $\text{Ni}_8\text{Bi}_8\text{SI}$.

The resistivity at 300 K ($30 \mu\Omega \text{ cm}$) for $\text{Ni}_8\text{Bi}_8\text{SI}$ is more than 1 order of magnitude lower than that reported for $\text{Ta}_4\text{Te}_4\text{M}$ ($\text{M} = \text{Cr}, \text{Fe}, \text{Co}, \text{Ni}$),^{5, 28} $\rho = 340\text{--}2300 \mu\Omega \text{ cm}$, indicating that $\text{Ni}_8\text{Bi}_8\text{SI}$ is a better conductor than low-dimensional Ta and Nb ternary tellurides. EH calculations²⁹ have shown that the conductivity in $\text{Ta}_4\text{Te}_4\text{Fe}$ is mainly provided by d-states of the interstitial Fe atoms. Our calculations at the DFT level for $\text{Ni}_8\text{Bi}_8\text{SI}$ show that the conductivity occurs through the whole Ni–Bi intermetallic system. Thus, the $\text{Ni}_8\text{Bi}_8\text{SI}$ columns can be regarded as “molecular wires”. The susceptibility value for $\text{Ni}_8\text{Bi}_8\text{SI}$ ($\chi = 6.5 \times 10^{-5} \text{ emu/g}$) is 3–10 times higher than those reported for $\text{Ta}_4\text{Te}_4\text{M}$ ($\text{M} = \text{Cr}, \text{Fe}, \text{Co}, \text{Ni}$).⁵

The analysis of difference charge densities reveals the most important interactions between metal atoms to be multicenter in character, corresponding to Ni–Bi rather than Ni–Ni bonds. Classical pairwise Ni–S interactions were also detected. The difference of the $\Delta\rho$ maxima shapes (see above) seems to be caused by the distortion of the $[^1_{\infty}\text{Ni}_8\text{Bi}_8\text{S}]$ columns. Finally, a number of quite weak electrostatic interactions between the I^- anions and positively charged 1D columns hold the structure elements together.

(29) Li, J.; Hoffmann, R.; Badding, M. E.; DiSalvo, F. J. *Inorg. Chem.* **1990**, *29*, 3943.

Noticeably, $\text{Ni}_8\text{Bi}_8\text{SI}$ and $\text{Ta}_4\text{Te}_4\text{E}$ differ by the nature of the d-element. The late transition metal, Ni, has more valence d-electrons than the early transition metal, Ta. Consequently, whereas in $\text{Ta}_4\text{Te}_4\text{E}$ the interstitial element provides the electrons to stabilize the structure, in $\text{Ni}_8\text{Bi}_8\text{SI}$ the interstitial element, sulfur, and the surrounding iodine serve as electron sinks withdrawing the excess electrons from the intermetallic Ni–Bi core.

Conclusion

$\text{Ni}_8\text{Bi}_8\text{SI}$ provides a new type of a quasi-one-dimensional conductor constructed of “molecular wires” separated by iodine. It exhibits physical properties typical for one-dimensional compounds. Being made of the 1D infinite, charged columns $[^1_{\infty}\text{Ni}_8\text{Bi}_8\text{S}]^+$ and I^- ions, it displays a strong anisotropy in its band structure and electrical properties corresponding to a 1D metal with Pauli paramagnetism of conducting electrons. These properties are in good agreement with the results of the electronic structure calculations.

It can be expected that $\text{Ni}_8\text{Bi}_8\text{SI}$ is the first member of a larger series of one-dimensional conducting compounds based on late transition metals. The search for new members of the family is underway.

Acknowledgment. The authors thank Prof. K. V. Rao and Dr. L. Belova (KTH, Sweden) for the magnetic measurements. This work was supported by the Russian Foundation for Basic Research (RFBR, Grant No. 00-03-32647a) and the INTAS program (Grant No. 99-1672).

Supporting Information Available: X-ray crystallographic file for $\text{Ni}_8\text{Bi}_8\text{SI}$ (CIF). This material is available free of charge via the Internet at <http://pubs.acs.org>.

JA0167001